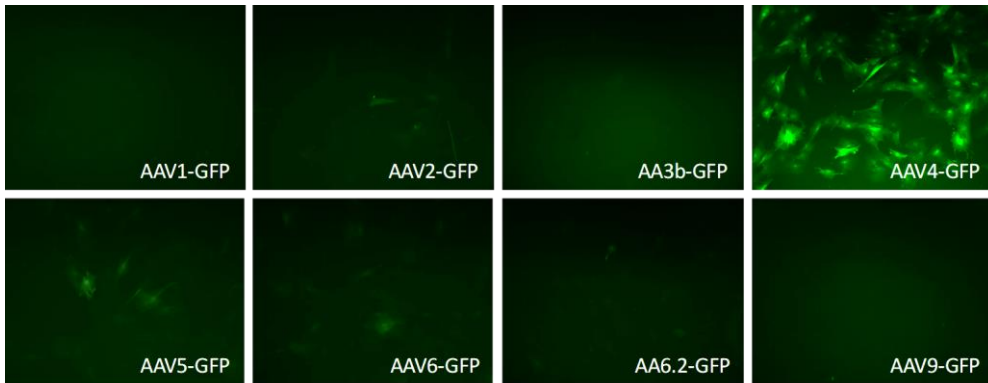
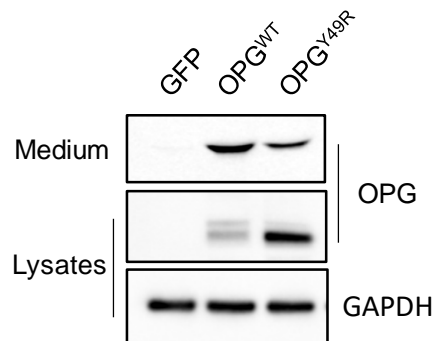


**RANKL-targeted combination therapy with osteoprotegerin variants  
devoid of TRAIL binding exerts biphasic effects on skeletal  
remodeling and anti-tumor immunity**

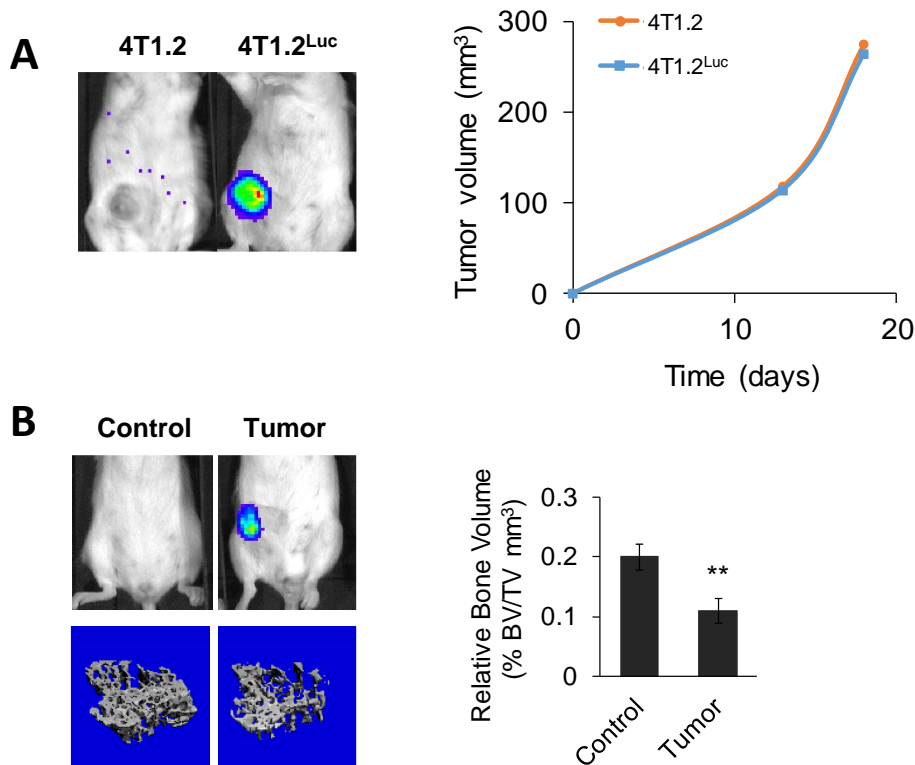
**SUPPLEMENTARY FIGURES**

Human	ET FPP KY LHY DE ETS HQ LLC DK CPP GT YLK QH CTA KW <b>KTVCA</b> <b>PCPDH</b> <b>Y</b> <b>Y</b> <b>T</b> <b>DSWHT</b> <b>SDECL</b> 60
Chimpanzee	ET FPP KY LHY DE ETS HQ LLC DK CPP GT YLK QH CTA KW <b>KTVCA</b> <b>PCPDH</b> <b>Y</b> <b>Y</b> <b>T</b> <b>DSWHT</b> <b>SDECL</b> 60
Mouse	ET LPP KY LHY DP ETG HQ LLC DK CAP GT YLK QH CT VRR <b>KTL</b> <b>CV</b> <b>PCPDH</b> <b>S</b> <b>Y</b> <b>T</b> <b>DSWHT</b> <b>SDECL</b> 60
Rat	ET FPP KY LHY DP ETG RQ LLC DK CAP GT YLK QH CT VRR <b>KTL</b> <b>CV</b> <b>PCPDY</b> <b>S</b> <b>Y</b> <b>T</b> <b>DSWHT</b> <b>SDECL</b> 60
Hedgehog	DN FAP KY LHY DP ETS RQ LMC DQ CPP GT FLK QH CTG KR P <b>TL</b> <b>CD</b> <b>PCPAH</b> <b>Y</b> <b>Y</b> <b>T</b> <b>DSWHT</b> <b>SDECL</b> 60
Rabbit	ET LPP KY LHY DP ETS RQ LMC DK CPP GT YLK QH CTA RR <b>E</b> <b>TL</b> <b>CT</b> <b>PCPDH</b> <b>Y</b> <b>Y</b> <b>T</b> <b>DTWHT</b> <b>SEDECL</b> 60
Dolphin	ET FPP KY LHY DP DTS RQ LLC DK CPP GT SLK QH CTA RR <b>KTL</b> <b>CA</b> <b>PCPDH</b> <b>Y</b> <b>Y</b> <b>T</b> <b>DSWHT</b> <b>SDECL</b> 60
Horse	ET FPP KY LHY DP ETS RQ LMC DK CPP GT FLK QH CTA RR <b>KTV</b> <b>CA</b> <b>PCPDH</b> <b>Y</b> <b>Y</b> <b>T</b> <b>DTWHS</b> <b>SDECL</b> 60
Cat	ET FPP KY LHY DP ETS RQ LMC DK CPP GT FLK QH CTA RQ <b>KTV</b> <b>CA</b> <b>PCPNH</b> <b>Y</b> <b>Y</b> <b>T</b> <b>DKWHT</b> <b>SDECL</b> 60
Dog	ET FPP KY LHY DP ETS RQ LMC DK CPP GT SLK QH CTA KR <b>KTV</b> <b>CV</b> <b>PCPNH</b> <b>Y</b> <b>Y</b> <b>T</b> <b>DLWHT</b> <b>SDECL</b> 60
Cow	ET FPP KY LHY DP ESS RQ LMC DK CPP GT FLK QP CTA RR <b>KTV</b> <b>CA</b> <b>PCPDH</b> <b>Y</b> <b>Y</b> <b>T</b> <b>DTWHT</b> <b>SDECL</b> 60
Pig	ET FPP KY LHY DP ETS RQ LMC DK CPP GT SLK QH CTA RR <b>KTV</b> <b>CA</b> <b>PCPDH</b> <b>Y</b> <b>Y</b> <b>T</b> <b>DSWHT</b> <b>SDECL</b> 60
Goat	ET FPP KY LHY DP ESS RQ LMC DK CPP GT FLK QP CTA RR <b>KTV</b> <b>CA</b> <b>PCPDH</b> <b>Y</b> <b>Y</b> <b>T</b> <b>DTWHT</b> <b>SDECL</b> 60
Sheep	ET FPP KY LHY DP ESS RQ LMC DK CPP GT FLK QP CTA RR <b>KTV</b> <b>CA</b> <b>PCPDH</b> <b>Y</b> <b>Y</b> <b>T</b> <b>DTWHT</b> <b>SDECL</b> 60
Turtle	ET SPP KY LHY DP VTS RQ LMC DL CPP GT YVK QH CTA AR <b>KTE</b> <b>CA</b> <b>PCPDQ</b> <b>Y</b> <b>Y</b> <b>AED</b> <b>WNSN</b> <b>DECQ</b> 60
Chicken	-- -- PPKY LHY DP GTS RQ VMC NQ CPP GS YVK QH CTA AS P <b>TV</b> <b>CA</b> <b>PCPDQ</b> <b>Y</b> <b>Y</b> <b>AED</b> <b>WNSN</b> <b>DECQ</b> 57
Lizard	----- KF PHY DP MTS RQ LMC DQ CPP GT YVK QN CTA SS <b>KT</b> <b>CS</b> <b>PCPDQ</b> <b>Y</b> <b>Y</b> <b>ADD</b> <b>WNSNE</b> <b>ECQ</b> 55
Zebrafish	----- YRRK DP ETG RT LEC AR CAP GS RLR QH CSS SRQ <b>TE</b> <b>CS</b> <b>PCG</b> <b>P</b> <b>G</b> <b>M</b> <b>Y</b> <b>T</b> <b>E</b> <b>F</b> <b>W</b> <b>N</b> <b>Y</b> <b>I</b> <b>P</b> <b>D</b> <b>C</b> <b>L</b> 54
Xenopus	----- LQC DQ CPP GMYVK QD CTT ER <b>KTE</b> <b>CA</b> <b>PCPAH</b> <b>Y</b> <b>Y</b> <b>S</b> <b>DM</b> <b>W</b> <b>D</b> <b>S</b> <b>N</b> <b>T</b> <b>E</b> <b>C</b> <b>N</b> 43

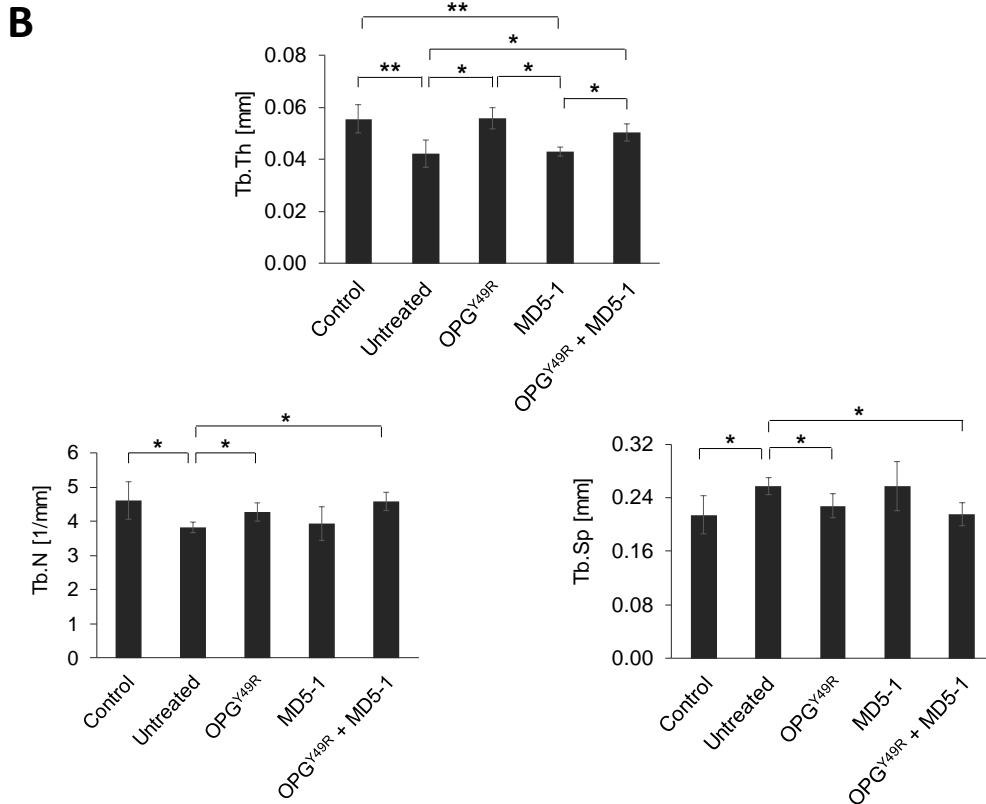
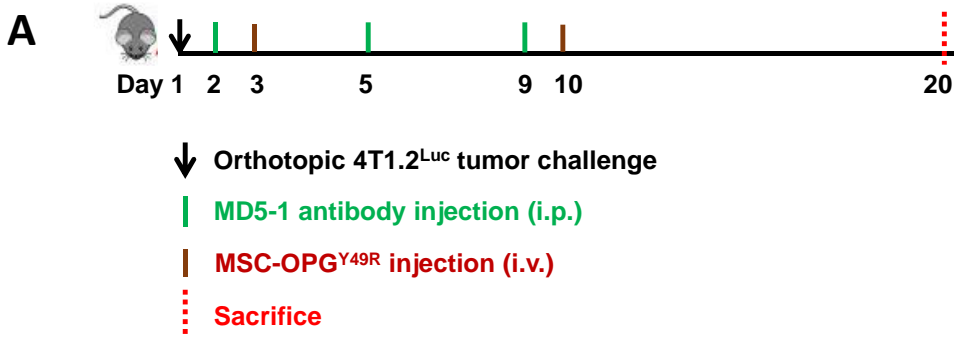
**Supplementary Figure S1: Aromatic residue Y49 in human OPG is conserved in all vertebrate species.** Sequences of OPG from different species were compared using Multiple Sequence Alignment (Clustal W). The conserved tyrosine residue (Y) is highlighted in green box across different organisms.

**A****B**

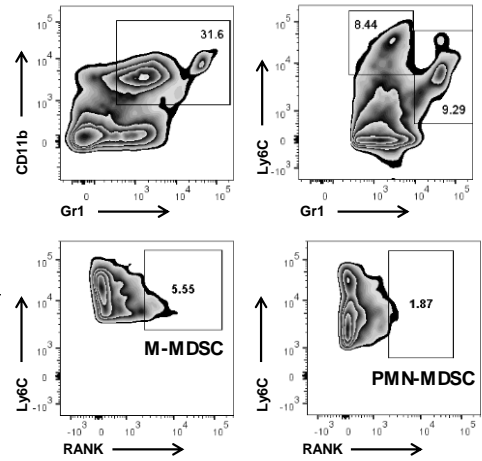
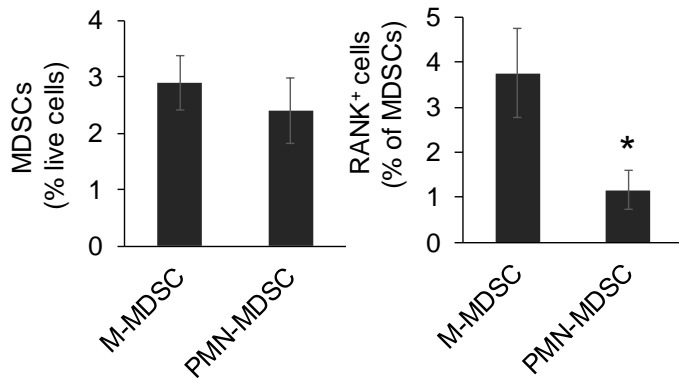
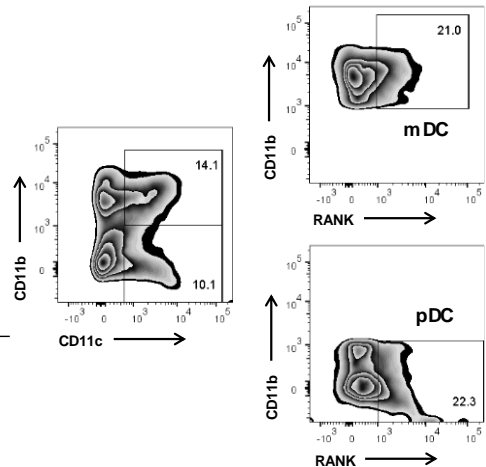
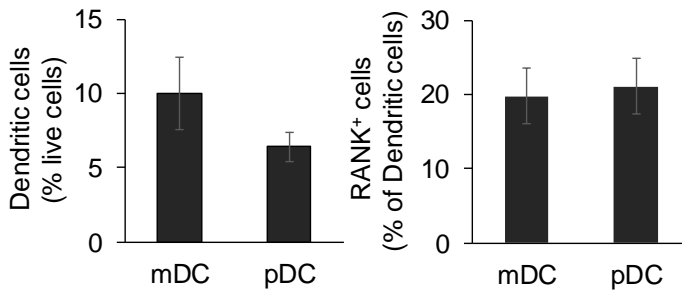
**Supplementary Figure S2: Transduction efficiency of AAV serotype capsids on mouse MSCs.** **A)** Different AAV serotype capsids containing GFP transgene were tested for their ability to transduce MSCs from BALB/c mouse. Briefly, MSCs were plated in 60 mm dishes at a density of  $4 \times 10^5$ . Next day, the cells were infected with rAAV-GFP ( $1 \times 10^5$  vector particles/cell) and cultured for 2 days and GFP expression was observed using a fluorescent microscope and images were taken (10x). The results indicated that AAV serotype-4 capsid possesses highest transduction efficiency in mouse MSCs. **B)** Following the above identification, rAAV expressing either wild type (rAAV-OPG<sup>WT</sup>) or mutant OPG (rAAV-OPG<sup>Y49R</sup>) were packaged and purified in serotype-4 capsids. The vectors were transduced to MSCs and the cell lysates and conditioned media were prepared after 48 hrs and analyzed by Western blotting for expression and extracellular secretion of OPG protein, respectively.



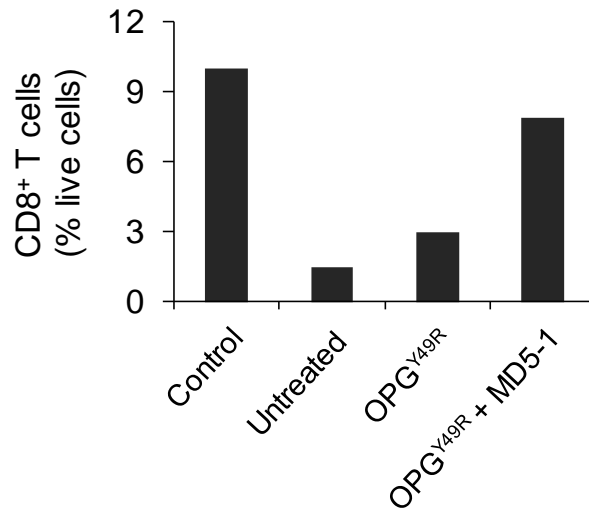
**Supplementary Figure S3: Development and characterization of 4T1.2<sup>Luc</sup> cell line, constitutively expressing firefly luciferase.** **A)** Parental 4T1.2 cells were transduced with a recombinant lentiviral vector expressing luciferase and resistant clones were selected using puromycin. Positive clones were expanded and equal amount of 4T1.2 and 4T1.2<sup>Luc</sup> cells were subcutaneously injected into female BALB/c mice and luciferase expression was monitored by non-invasive luciferase imaging (left panel). Tumor growth kinetics was measured using a digital caliper and tumor volume is shown on the right panel. **B)** To establish an osteolytic breast cancer model, 4T1.2<sup>Luc</sup> cells were injected into the 4<sup>th</sup> mammary fat pad of eight-week-old female BALB/c mice. Primary and secondary tumor development was monitored using non-invasive IVIS imaging. Bone damage was examined on day-18 by micro-CT. Data from micro-CT were used in 3D reconstruction images. Representative images from luciferase imaging and micro-CT (left panel) and quantitative analysis of respective bones for bone volume (right panel) are shown. \*\*,  $P < 0.01$ .



**Supplementary Figure S4: Systemic cell therapy with OPG<sup>Y49R</sup> restores bone architecture.** **A)** The overall experimental schema - female BALB/c mice were implanted with 4T1.2<sup>Luc</sup> cells. Days of MD5-1 antibody and MSC-OPG<sup>Y49R</sup> treatment and endpoint sacrifice are shown. **B)** Upon sacrifice of mice on day-20, tibiae were processed for evaluation of bone architecture by micro-CT. Data obtained from micro-CT scans were used for quantitative analysis of bone volume (BV, data shown in **Fig. 3B**), trabecular thickness (Tb. Th), trabecular number (Tb. N), and trabecular separation (Tb. Sp), \*,  $P < 0.05$ ; \*\*,  $P < 0.01$ .

**A****B**

**Supplementary Figure S5: RANK expression on immune cells.** **A and B**, Twenty days after orthotopic inoculation of 4T1.2<sup>Luc</sup> cells in female BAL/c mice, mice were sacrificed and tumor tissues explanted. Single-cell suspensions of explanted tumors were analyzed for macrophages (data shown in **Fig. 4A**), MDSCs (**A**), DCs (**B**) and RANK expression in respective population by flow cytometry. For MDSC, CD11b<sup>+</sup>Gr1<sup>+</sup> cells were further gated as Ly6C<sup>high</sup> (M-MDSC) and Ly6C<sup>low</sup> (PMN-MDSC) subtypes. For DCs, CD11c<sup>+</sup> cells were further gated as CD11b<sup>+</sup> (mDC) and CD11b<sup>-</sup> (pDC) subtype. RANK expression within MDSC and DC populations was analyzed using a PE-conjugated anti-RANK antibody. Relative percentages of MDSCs or DCs and RANK expression among them are shown in bar graph in the left panel and gating strategy is shown in right panel.



**Supplementary Figure S6: Combination therapy with OPG<sup>Y49R</sup> and MD5-1 improves CD8<sup>+</sup> T cells.** Twenty days after initiation of indicated treatment combinations, mice were sacrificed and CD3<sup>+</sup>CD8<sup>+</sup> T cells were enumerated by flow cytometry. Data indicated represents total CD8<sup>+</sup> T cells within total live cells.